Accepted Manuscript

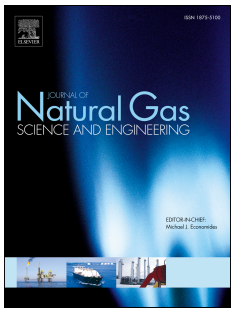

A prediction model of the accumulation shape of insoluble sediments during the leaching of salt cavern for gas storage

Jinlong Li, Xilin Shi, Tongtao Wang, Chunhe Yang, Yinping Li, Hongling Ma, Xuqiang Ma, Hui Shi

PII: S1875-5100(16)30406-1

DOI: 10.1016/j.jngse.2016.06.023

Reference: JNGSE 1570

To appear in: *Journal of Natural Gas Science and Engineering*

Received Date: 16 March 2016

Revised Date: 29 May 2016

Accepted Date: 7 June 2016

Please cite this article as: Li, J., Shi, X., Wang, T., Yang, C., Li, Y., Ma, H., Ma, X., Shi, H., A prediction model of the accumulation shape of insoluble sediments during the leaching of salt cavern for gas storage, *Journal of Natural Gas Science & Engineering* (2016), doi: 10.1016/j.jngse.2016.06.023.

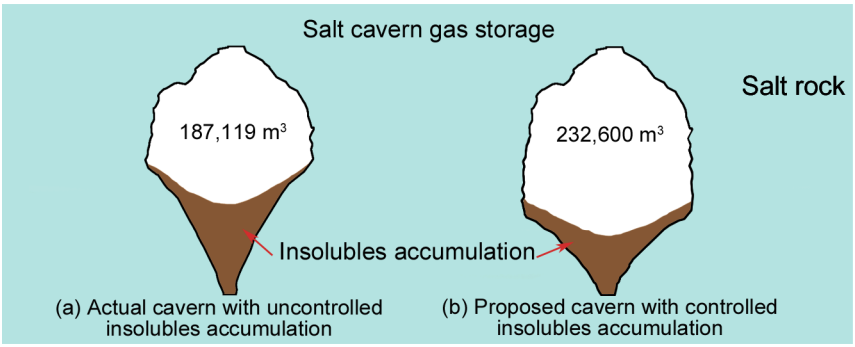

A prediction model of the accumulation shape of insoluble sediments during the leaching of salt cavern for gas storage

Jinlong Li*, Xilin Shi, Tongtao Wang*, Chunhe Yang, Yinping Li, Hongling Ma, Xuqiang Ma, Hui Shi

State Key Laboratory of Geomechanics and Geotechnical Engineering, Institute of Rock and Soil Mechanics, Chinese Academy of Sciences, Wuhan 430071, Hubei, China

Abstract: A mathematical model is proposed to predict the accumulation shape of the insoluble sediments during cavern leaching. Laboratory tests have been carried out to determine the properties affecting the shape of the insolubles accumulation. The cutoff value of insoluble substances content in rock salt is introduced in the mathematical model. The equations of the shape of the insolubles accumulation are deduced, and a computer program is developed based on these equations. JT-52 cavern of Jintan salt mine is simulated by the program. The simulation results are compared with the sonar survey data of the insolubles accumulation shape of JT-52 cavern to verify the accuracy of the mathematical model. It shows that the proposed mathematical model has a high accuracy, which can satisfy the requirement of the actual engineering. A smaller distance between the inner leaching tubing and the blanket is suggested in the early leaching stages to increase the usable volume of the cavern.

Keywords: Underground gas storage; Salt cavern; Mathematical model; Cavern

*Corresponding author at: State Key Laboratory of Geomechanics and Geotechnical Engineering, Institute of Rock and Soil Mechanics, Chinese Academy of Sciences, Wuhan 430071, Hubei, China. Email: oklijinlong@126.com (Jinlong Li); ttwang@whrsm.ac.cn (Tongtao Wang)

leaching; Insolubles accumulation shape

Nomenclature

BS interface	Brine-Sediment interface
SS interface	Salt-Sediment interface
D	base length of the insolubles triangle
h	height of the insolubles produced per unit step
h_{sum}	height of the insoluble sediments
$h_{\Delta}(n)$	height of the n^{th} triangle
H_0	height of the initial cavern wall
H_M	height of cavern wall at x_M
H_N	height of wall-N
H_r	maximum release height of the insoluble particles
H_x	height of the cavern wall
ΔH_x	height of the additional part of the dissolved cavern roof
k	slope of the BS interface
m_x	number of the accumulated triangles
r_0	distance between the coordinate origin and the symmetry axis of the cavern
$S_{\Delta \mathrm{ABE}}$	area of the insoluble triangle
t	thickness of the dissolved cavern wall per unit step
V	volume of insoluble substances produced per unit step
x_M	x-coordinate of point M
x_N	x-coordinate of wall-N
y_{BS}	y-coordinate of the BS interface
$y_{BS}{}'$	derivative of the BS interface equation
y_N	y-coordinate of the SS interface on wall-N
y_{SS}	y-coordinate of the SS interface
$y_{SS}{}^*$	increased height of the SS interface in one unit time step
γ	a scattering coefficient
ϵ	expansion coefficient of the insoluble substances in brine
θ	angle of repose of insoluble sediments in the brine
μ	content of insoluble substances in the rock salt
μ_0	cutoff value of the insolubles content in the rock salt

[Reviewer #1, (1)]

1 Introduction

Underground gas storage (UGS) is accepted as a strategic method to shave the fluctuation of the supply-demand of natural gas throughout the year, and even a day (Arfaee and sola, 2014; Wang et al., 2015a). Among various kinds of UGSs, salt cavern gas storage is one of the most favorable options (Wang et al., 2015b), because of its excellent injection and delivery capacities (Chen et al., 2013; Li et al., 2014; Yang et al., 2015). Due to the easy water solubility of rock salt, water solution mining is widely used to construct salt cavern UGSs (Liu et al., 2015; Zhang et al., 2014). Water or unsaturated brine is injected through a well drilled into a salt bed to leach a void or cavern, and the brine is expelled until the completion of the cavern (Shi et al. 2015). Rock salt contains insoluble substances, which detach from the cavern wall and fall down to the cavern bottom during the cavern leaching (Ma et al., 2015). These sediments seriously inhibit lower cavern growth and reduce the usable volume of the cavern. In addition, they may cause flow restrictions or tube plugging unless being controlled or removed (Warren, 2006). To facilitate the description, we defined the top and bottom surfaces of the insolubles accumulation as the Brine-Sediment interface (BS Interface) and Sediment-Salt interface (SS interface) respectively, which are presented in Fig. 1. The BS interface is the interface between the brine and the insoluble sediments, which can be observed by a Sonar survey. It is the ultimate boundary of the gas storage and its shape has notable effects on the usable volume of the cavern. The SS interface is the interface between the insoluble sediments and the in-situ rock salt. Two main effects of the shape of the insolubles accumulation on the

salt cavern UGS are as follows:

(i) Affect the volume of the cavern and the use efficiency of salt beds. Fig. 1 presents the shape of cavern JT-101 of Jintan salt mine, Jiangsu province, China, with different slope angle SS interfaces. As shown in Fig. 1a, this cavern was created from the starting point at a depth of -1050 m to the ending point at a depth of -990 m. The lowest point of the completed cavern is at a depth of -1024 m. The insoluble sediments raise the cavern bottom from -1050 m to -1024 m, which means that the height of the insoluble sediments is 26 m and the effective height of the cavern is only 34 m. Based on the field data, the volume of the insoluble sediments accounts for only about 16.5% of the total cavern volume, while the height of the insoluble sediments accounts for as much as 43% of the total cavern height. The total usable volume of the cavern was decreased greatly, which resulted from the fact that the insolubles accumulation shape is not well controlled. The slope of the SS interface is too large (about 75 degrees) which results in the cavern having a high bottom. Fig. 1b presents the shape of the cavern with a low slope angle SS interface (about 45 degrees). The bottom of the cavern is reduced to about -1033 m, and the usable volume of the cavern is increased by about 25% compared with that of the cavern in Fig. 1a. This confirms that decreasing the slope angle of the SS interface is an effective method to improve the cavern volume and salt formation use efficiency.

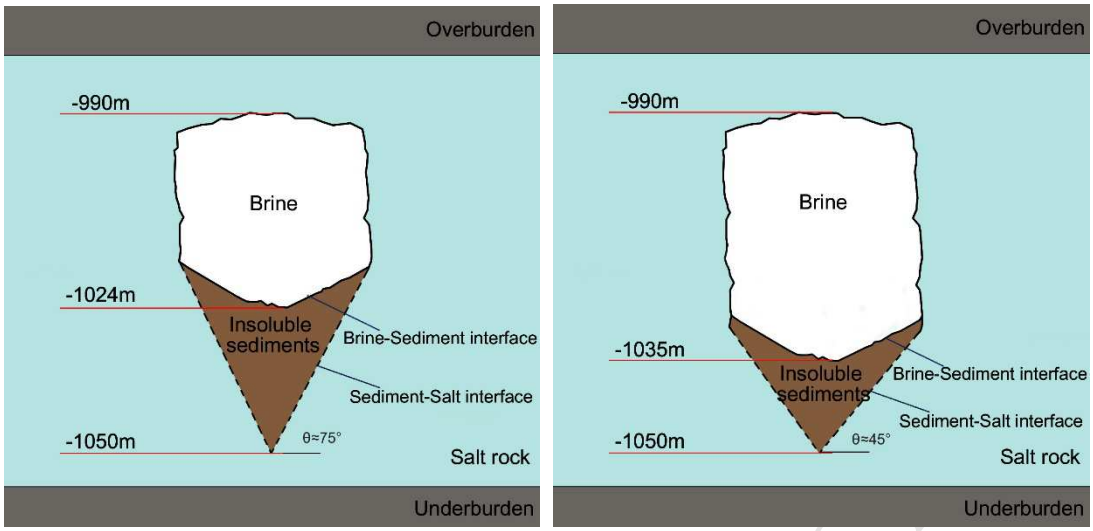

(a) **(b)**

Fig. 1. Caverns JT-101 of Jintan salt mine, Jiangsu province, China, with different insolubles slope angles. (a) Cavern with high-slope angle SS interface. (b) Cavern with low-slope angle SS interface.

(ii) Affect the volume use efficiency of the leached cavern. Fig. 2 presents the vertical section of the Cavern EZ16, at Etrez, France (Charnavel and Lubin, 2002). The BS interface of Cavern EZ16 has a high center, at -1455 m, while the depth of the brine bottom is at -1475 m. When the brine is being expelled by the gas, the de-brining pipe can only reach the top of the BS Interface. This means that all the brine below -1455 m can not be replaced by gas. This caused about 10 % of the volume available for gas storage to be lost (Charnavel and Lubin, 2002).

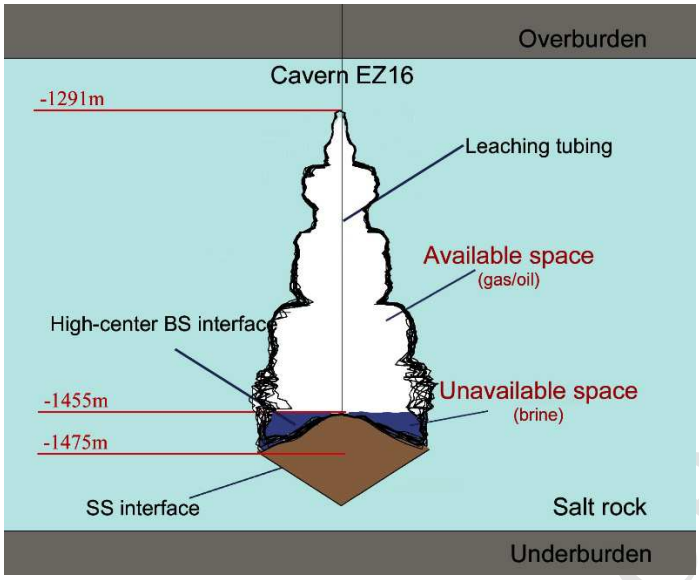

Fig. 2. Vertical section of the Cavern EZ16, Etrez, France (Charnavel and Lubin, 2002).

Many researchers have done many constructive works on cavern shape design and control during leaching. Durie and Jessen (1964) studied the control mechanism of cavern shape by physical simulation experiments, and proposed an experience formula of salt rock solution rate. Nolen et al. (1974) numerically simulated the cavern leaching process, in which the cavern shape and cavern volume increase rate were predicted. Reda and Russo (1986) simulated the process of cavern leaching in the laboratory and obtained a cylindrical cavern. Quintanilha and Nguyen-Minh (1994) proposed an optimized cavern shape design, in which the cavern shape, temperature gradient, and creep were considered. Staudtmeister and Rokahr (1997) thought that the salt cavern with a shape of slender cylinder was good for the stability. Charnavel and Lubin (2002) found the bottom shapes of several caverns could not be explained by current cavern leaching theory or cavern leaching software. He added to the Gaz de France leaching code a procedure of the cavern floor shaping during leaching to solve this problem. The BS interface was included, but the effects of the formation and development of the SS

interface were neglected. Willson et al. (2004) built a model to predict the cavern shape, which took into consideration the concentration of the injected liquid, injection rate and the dissolution rate of salt. Sobolik and Ehgartner (2006) studied the safety factor, volume shrinkage, displacement, and ground subsidence of salt cavern gas storages with shapes of cylinders, enlarged top, enlarged middle, and enlarged bottom by numerical simulations. von Tryller and Musso (2006) proposed a method for controlling cavern leaching in bedded salt without blanket. Wang et al. (2013) proposed a new model to design the shape of salt cavern gas storage, and introduced the concepts of slope instability and pressure arch. Most of the studies only considered cavern form control in pure rock salt and neglected the effects of the insolubles. This results in that there are large differences between the shapes of the actual and designed caverns. Most salt formations in China contain more than 15% insoluble substances, and the insoluble sediments in a single cavern can reach up to 40 meter high. The presence of high levels of insolubles has seriously held back the cavern development, which is worthy of more attention.

The main motivation of this paper is to propose a mathematical model for the prediction of the accumulation shape of the insoluble sediments. To obtain the parameters used in the mathematical model, experiments have been carried out. Based on reasonable hypotheses and simplifications, theoretical formulas of the shape of the insolubles accumulation are deduced. A computer program is developed based on these formulas. Simulation results are compared with the actual cavern shape to verify the proposed prediction model. Suggestions on decreasing the adverse impact of the

insoluble substances on the shape and usable volume of the cavern are given based on the results.

2 Experiments and analysis

During cavern leaching, the salt is dissolved into brine while the insoluble particles detach from the cavern side-wall and fall down to the bottom of the cavern. The falling of the insoluble particles is affected by impacting on the cavern side-wall and accumulation of the insolubles on the cavern bottom reduces the dissolution rate of rock salt and reshapes the cavern side-wall. To figure out how the insoluble particles interact with the cavern side-wall, experiments are carried out. [Reviewer #3, (1)] In Section 2.1, insoluble particles falling experiments are described that have been carried out to find out the falling rule of the insoluble particles under the influence of the cavern side-wall. In Section 2.2, rock salt dissolution experiments are reported that have been carried out to figure out the impact of these insoluble particles on the dissolution of cavern side-wall. These experiments provide the parameters and basis to establish the mathematical model in Section 3.

2.1. Insoluble particles falling experiment

At each moment during cavern leaching, a number of insoluble particles lose support and fall into the brine in the cavern. Ultimately they accumulate at the cavern bottom. These particles have irregular shapes. During the falling in brine, the insoluble particles are affected by the turbulence forces, hydrodynamic counterforce, and occasional impact force on the salt-wall, etc. These factors result in the falling paths of

the insoluble particles being variable and difficult to predict. However, if the insolubles that fall over a given period are considered as a whole, the accumulation configurations of these insolubles assemblies in each period are similar. To determine the accumulation configuration of the insoluble particles in any given period, insoluble particles falling experiments are developed and carried out.

Fig. 3 presents the experimental arrangement and results. The water tank is made of transparent plexiglass to allow observing the falling traces of the particles. The tank is 60 cm long, 2 cm wide and 100 cm high, and is full of saturated brine during the tests. The temperature stays at 25 °C during the experiments. The original sample of insoluble particles, i.e. without further separation or selection, obtained from Jintan salt mine, is used in the tests. The sample is divided into ten equal parts, which are released at distances of 10 cm, 20 cm, 30 cm, 40 cm, 50 cm, 60 cm, 70 cm, 80 cm, 90 cm and 100 cm above the bottom of the water tank to simulate the falling of insoluble particles in salt cavern from different heights (Fig. 3a). During the experiments, we observed the particles falling like a dead leaf. When a non-spherical particle is set free in liquid, it drifts and rotates to the center of the channel as it falls down (Hu et al., 1992; Feng and Joseph, 1994). The lateral drift magnitudes of the insoluble particles are varied, for the insoluble particles have various shapes. The insolubles settle over a distance to the sidewall. Those who are released from higher position settle over a larger distance from the side-wall than those released from a lower position, as shown in Fig. 3b. These insolubles released from different height approximately form a triangular shape in the tank bottom. Fig. 3c presents the results of the experiment. We

repeat the experiment three times, and the fallen particles form a triangle in each trial.

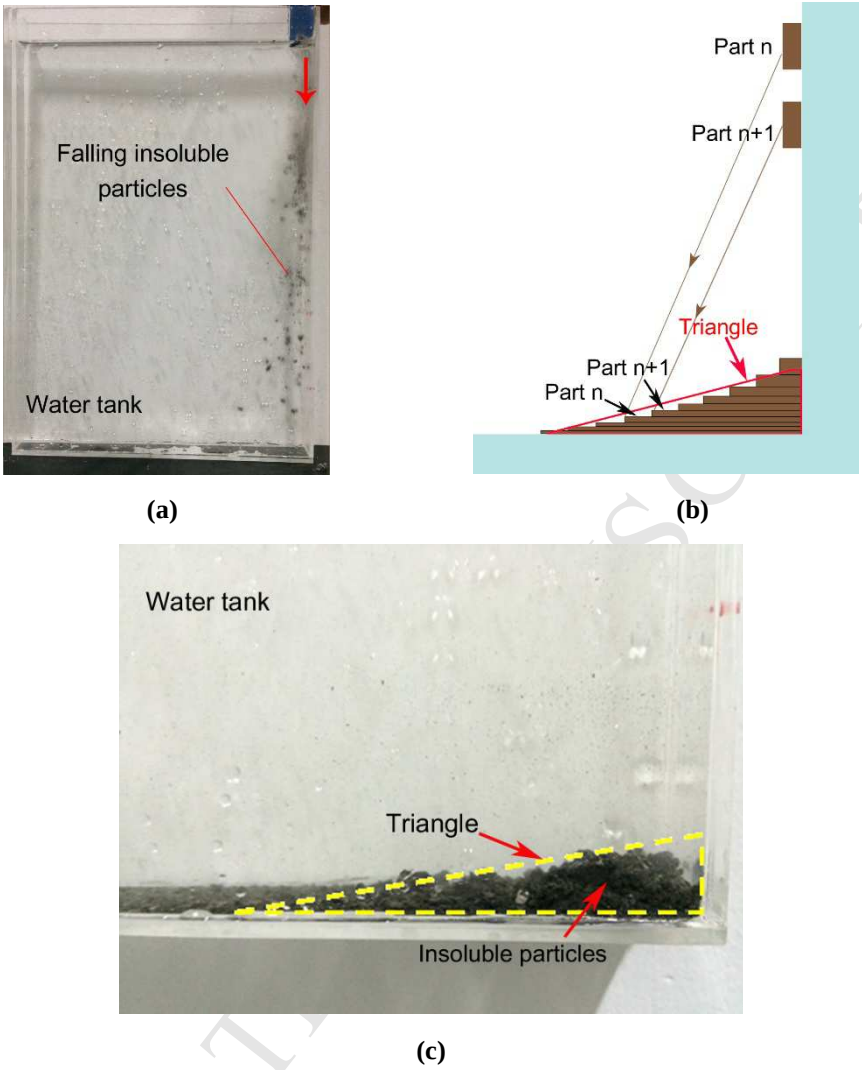

Fig. 3. Results of the experiment on the falling of insoluble particles. (a) Falling insoluble particles. (b) Distribution of the insolubles fallen from different heights. (c) Results of the falling experiments.

The horizontal length of the triangle is related to the maximum release height of the particles. To obtain their quantitative relationships, a series of experiments with different maximum release heights have been performed under the same conditions. The horizontal length of the triangle is measured. Fig. 4 shows the relationship between the horizontal base length of the insoluble triangle and the maximum release height of the insoluble particles. The data are fitted into a linear function, which has a high fitting

degree (R^2 in Fig. 4) up to 0.9725.

Therefore, it can be concluded that

$$D = \gamma H_r \quad (1)$$

where D is the base length of the insolubles triangle; H_r is the maximum release height of the insoluble particles; γ is the scattering coefficient between D and H_r.

The value of γ is about 0.0798 in this experiment on the particles from Jintan salt mine.

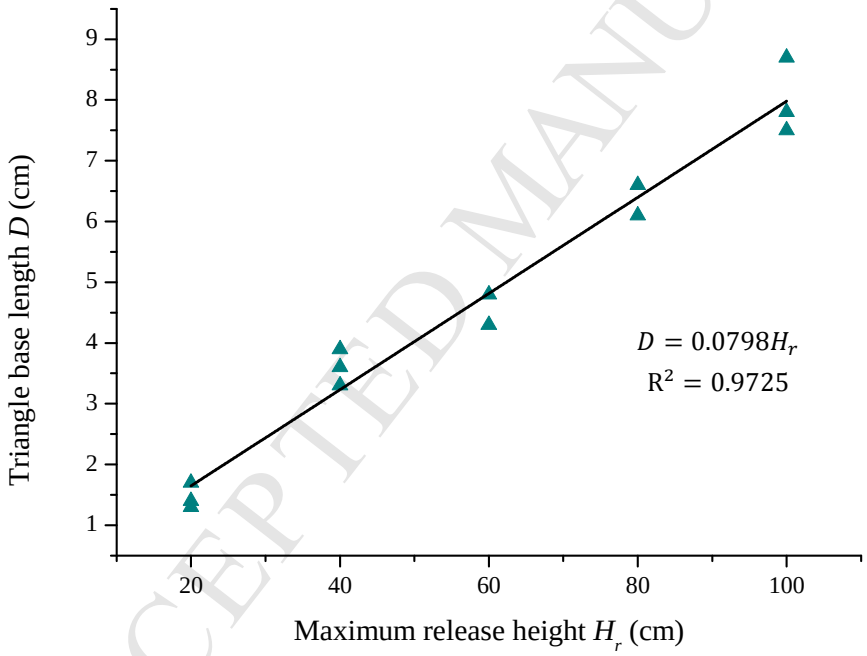

Fig. 4. Relationship between the triangle base length and the maximum release height of the insoluble particles.

2.2. Rock salt dissolution experiment

The accumulation of the insoluble particles reduces the contact area between the brine and the salt, affecting the dissolution of the rock salt. To quantitatively determine the influence of the accumulation of insoluble particles on the dissolution

of rock salt, a rock salt dissolution experiment has been designed. Fig. 5a presents a brick-shaped sample of rock salt placed in a transparent plexiglass tank, with part of its surface covered by different sizes of insoluble particles from Jintan salt mine. The rock salt sample is almost pure salt with a salt content of 99.5%, and it is 10 cm long, 2 cm wide and 20 cm high. The water tank is about 20 cm × 10 cm × 10 cm. The insoluble particles are piled up into a triangular pyramid, and the interface between insolubles and the rock salt sample is a triangle. Fresh water is injected into the tank slowly, which ensures that the insoluble particles are not washed away (Fig. 5b). During the experiment, the temperature stays at about 25 °C.

After about 30 minutes, the water is pumped out and the sample is taken out. The exposed regions of the sample are dissolved to about 4 mm depth, as shown in Fig. 5c. The regions covered by the insoluble particles, as highlighted in red in Fig. 5c, are not dissolved at all. As the rock salt is covered by insoluble particles, the insolubles reduce the contact area between the brine and the salt wall, stopping the boundary layers from moving further. As the brine boundary layers gradually become saturated, the dissolution of the rock salt covered by insolubles will totally stop. In a real salt cavern, meters of insoluble particles are more compacted than those in the experiments. The dissolution of the rock salt covered by insolubles will also stop in this case. [Reviewer #3, (4)]. Therefore, that the rock salt covered by the insolubles stops dissolving is assumed in Section 3.1.

(a)

(b) **(c)**

Fig. 5. The water tank salt dissolution experiment. (a) Insolubles and salt sample before the water is injected. (b) After the water is injected. (c) Result of the experiment.

3 Mathematical model of the shape of the insolubles accumulation

3.1. Assumptions

Based on the experimental results in Section 2.1 and Section 2.2 and the observation of sonar detection, the assumptions are made that:

(i) Accumulation shape of the insoluble particles in one time step is approximately a triangle, whose base length is proportional to the distance from where the insolubles fall to where they accumulate.

(ii) Once the rock salt is covered with insolubles, its dissolution stops.

(iii) Cavern shape is axisymmetric.

(iv) Cavern side-wall remains vertical.

Based on the above assumptions, the equations of the BS interface and SS interface of the insolubles accumulation in salt cavern are deduced in Section 3.2.

3.2. Governing equations of insoluble interfaces

Due to the cavern top being protected by the blanket, the cavern is developed laterally most of the time. Considering the assumption that the cavern is axisymmetric and the cavern side-wall remains vertical, the development of the cavern can be simplified to a 2-D axisymmetric model. Fig. 6 presents a schematic diagram of the cavern leaching process. In the model, the development of the cavern is divided into N steps. For every step time, the rock salt of the cavern wall with a thickness t is dissolved.

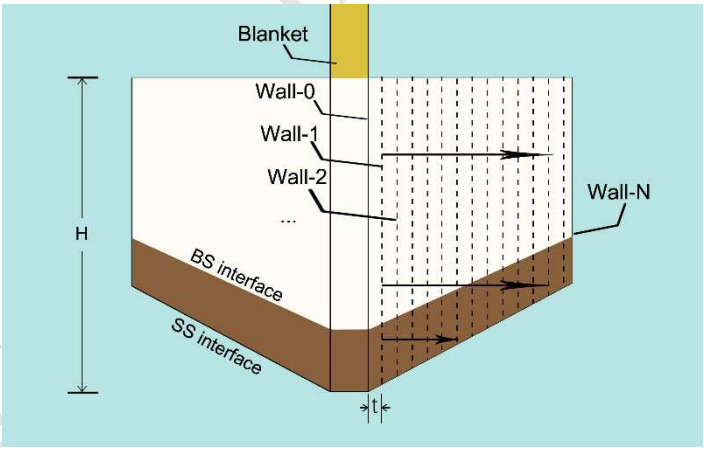

Fig. 6. Schematic diagram of the cavern leaching process.

Based on the experimental results of Section 2.1, the insoluble substances in the rock salt accumulate into a triangle shape in each unit step. Fig. 7 presents a sketch of the distribution of the insoluble substances after step one. The volume of insoluble

substances produced per unit step is

$$V = \mu\epsilon H_0 t \tag{2}$$

where V is the volume of insoluble substances produced per unit step; μ is the content of insoluble substances in the rock salt; ϵ is the expansion coefficient of the insoluble substances in brine, which considers the effects of broken expansion and compaction; [Reviewer #3, (2)]. H_0 is the height of the initial cavern wall on wall-0; and t is the thickness of the dissolved cavern wall per unit step.

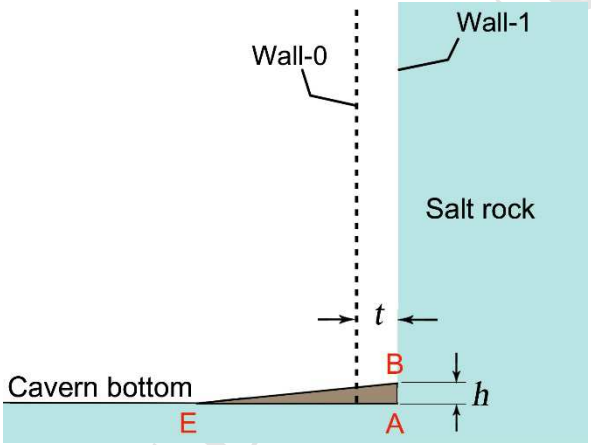

Fig. 7. Sketch of the distribution of the insoluble substances after step one.

V is also equal to the product of the area of ΔABE and unit thickness (usually valued as 1). Since the length of $|AE|$ is γH_0, the length of $|AB|$ can be written as

$$h = \frac{2S_{\Delta ABE}}{\gamma H_0} = \frac{2V}{\gamma H_0} = \frac{2\mu\epsilon t}{\gamma} \tag{3}$$

where h is the height of the insolubles ($|AB|$ in Fig. 7); $S_{\Delta ABE}$ is the area of ΔABE.

According to the experimental results of Section 2.2, the rock salt covered by the insolubles will stop dissolving. Therefore, the dissolution of the side-wall will start from point B in the next unit step. The processes are repeated until the completion of the cavern leaching. The side-wall of the salt cavern moves to wall-N after N unit steps. Fig. 8 presents a sketch of the distribution of the insoluble substances after N steps.

The BS interface grows and gradually forms a smooth bottom. To facilitate describing the SS interface and the BS interface, a system of rectangular coordinates is introduced. A is set as the origin point and the positive directions of the system are marked in Fig. 8.

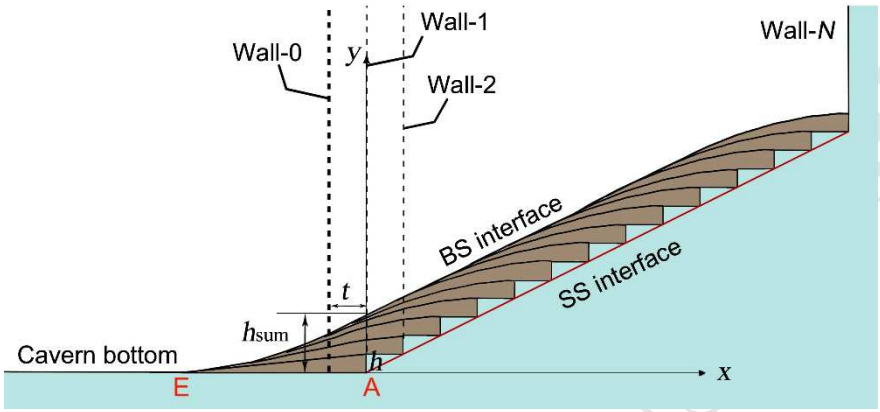

Fig. 8. Sketch of the distribution of the insoluble substances after *N* steps.

As can be seen from Fig. 8, the SS interface moves distance t to the right and h upward in each step. The SS interface is a straight line with slope h/t. Taking the value of h (Eq. (3)) into consideration, the equation of the SS interface can be written as

$$y_{SS} = \frac{2\mu\epsilon}{\gamma}x \tag{4}$$

where y_{SS} is the y-coordinate of the SS interface.

As shown in Fig. 8, the insolubles deposit is composed of many triangles. The number of the accumulated triangles can be expressed as

$$m_x = \begin{cases} \frac{\gamma H_x + x}{t} & (-\gamma H_0 \le x < 0) \\ \frac{\gamma H_x}{t} & (0 \le x < x_N - \gamma H_N) \\ \frac{x_N - x}{t} & (x_N - \gamma H_N \le x \le x_N) \end{cases} \tag{5}$$

where m_x is the number of the accumulated triangles at x; H_x is the height of the cavern wall at x; x_N is the x-coordinate of wall-N; and H_N is the height of wall-N.

The height of the n^{th} triangle at the same x-coordinate can be expressed as

$$h_{\Delta}(n)=\begin{cases} h\times\frac{\gamma H_x-[-x+(n-1)t]}{\gamma H_x} & (-\gamma H_0<x<0) \\ h\times\frac{\gamma H_x-(n-1)t}{\gamma H_x} & (0\le x\le x_N) \end{cases} \quad (n=1, 2, 3,\ldots, m_x) \quad (6)$$

where $h_{\Delta}(n)$ is the height of the n^{th} triangle.

Based on Eqs. (3), (5) and (6), the height of the insoluble sediments can be expressed as

$$h_{\mathrm{sum}}=\sum_{n=1}^{m_x}h_{\Delta}(n)=\begin{cases} \frac{\mu\epsilon(\gamma H_x+x)^2}{\gamma^2 H_x} & (-\gamma H_0<x<0) \\ \mu\epsilon H_x & (0<x<x_N-\gamma H_N) \\ \mu\epsilon H_x-\frac{\mu\epsilon(\gamma H_x-x_N+x)^2}{\gamma^2 H_x} & (x_N-\gamma H_N<x<x_N) \end{cases} \quad (7)$$

where h_{sum} is the height of the insoluble sediments at x.

Therefore, the equation of the BS interface can be written as

$$y_{BS}=y_{SS}+h_{\mathrm{sum}}=\begin{cases} \frac{\mu\epsilon(\gamma H_x+x)^2}{\gamma^2 H_x} & (-\gamma H_0<x<0) \\ \frac{2\mu\epsilon}{\gamma}x+\mu\epsilon H_x & (0<x<x_N-\gamma H_N) \\ \frac{2\mu\epsilon}{\gamma}x+\mu\epsilon H_x-\frac{\mu\epsilon(\gamma H_x-x_N+x)^2}{\gamma^2 H_x} & (x_N-\gamma H_N<x<x_N) \end{cases} \quad (8)$$

where y_{BS} is the y-coordinate of the BS interface.

Eqs. (4) and (8) are the equations of the SS interface and BS interface. The SS interface is a straight line whose slope is $\frac{2\mu\epsilon}{\gamma}$. Since the cavern top is flat, the height of the cavern wall is related to the height of the insoluble sediments, which is expressed as

$$H_x=H_0-y_{BS} \quad (9)$$

Thus, the main part of the BS interface ($0<\mathrm{x}<x_N-\gamma H_N$) is a straight line as well, and its function is written as

$$y_{BS}=\frac{2\mu\epsilon}{\gamma(1+\mu\epsilon)}x+\mu\epsilon H_0 \quad (10)$$

The slope of the BS interface should be less than or equal to the angle of repose of insoluble sediments in brine, viz., Eq. (11) is satisfied.

$$k = \frac{2\mu\epsilon}{\gamma(1+\mu\epsilon)} \leq tan\theta \quad (11)$$

where k is the slope of the BS interface; θ is the angle of repose of insoluble sediments in the brine.

When $k = \tan\theta$, a cutoff value of the insolubles content in the rock salt can be obtained, and is expressed as

$$\mu_0 = \frac{\gamma\tan\theta}{2\epsilon(1-\gamma\tan\theta)} \quad (12)$$

where μ_0 is the cutoff value of the insolubles content in the rock salt.

When $\mu < \mu_0$, $k < tan\theta$, the derived insoluble sediments shape is stable, and Eqs. (4) and (8) are the equations of the SS interface and BS interface. When $\mu > \mu_0$, the slope of the BS interface is larger than the slope angle of the insoluble sediments, thus the insolubles will slip down and redistribute. Therefore, the equations of the BS interface and the SS interface should be modified in this case.

According to the experimental results of Section 2.1, the value of γ is about 0.08 (Fig. 4). Based on literature (Chen et al., 2013), the angle of repose of rock salt (θ) is between 25 and 40 degrees and the expansion coefficient of the insoluble substances (ϵ) is about 1.5. It can be estimated that the cutoff value of the insolubles content (μ_0) is between 1.2% and 2.3%. In fact, the insoluble substances content of rock salt in China far exceeds this cutoff value in most cases. From an application point of view, this paper will focus on the case when $\mu > \mu_0$.

On the left of wall-1, where x < 0, the derivative of the BS interface equation is

$$y_{BS}{}' = \frac{2\mu\epsilon(\gamma H_x + x)}{\gamma^2 H_x} \quad (-\gamma H_0 < x < 0) \quad (13)$$

$y_{BS}{}'$ increases with x and

$$y_{BS}{}' = \begin{cases} \frac{2\mu\epsilon}{\gamma} > \tan\theta & (x = 0) \\ 0 < \tan\theta & (x = -\gamma H_0) \end{cases} \tag{14}$$

Therefore, there must be a point between $x = -\gamma H$ and $x = 0$, where $y_{BS}{}' = \tan\theta$. Mark this point as P, and draw a tangent line to the BS Interface. Fig. 9 shows a sketch of the distribution of the fallen insoluble substances when $\mu > \mu_0$, where Q is the joint point between the tangent line and the SS interface. The insoluble substances beyond line PQ will slip down and they will have a new top as line LM (Fig. 9). However, the total volume of the insoluble substances does not change

$$\mu\epsilon \frac{(H_M + H_0)x_M}{2} = (\frac{2\mu\epsilon}{\gamma} x_M)^2 (\frac{1}{\tan\theta} - \frac{1}{\frac{2\mu\epsilon}{\gamma}}) \tag{15}$$

where x_M is the x-coordinate of point M; H_M is the height of cavern wall at x_M.

The x-coordinate of point M is expressed as

$$x_M = \frac{\gamma^2 (H_M + H_0)}{8\mu\epsilon\cot\theta - 4\gamma} \tag{16}$$

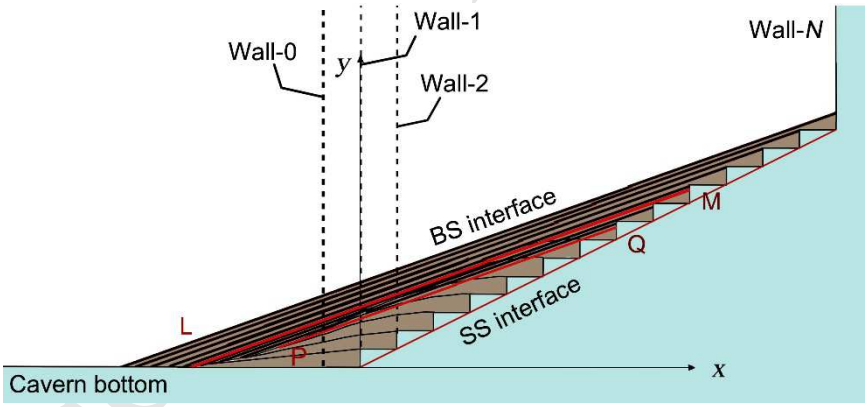

Fig. 9. Sketch of the distribution of the fallen insoluble substances when $\mu > \mu_0$.

To the left of point M, the equation of the SS interface is the same as when $\boldsymbol{\mu < \mu_0}$

$$y_{SS} = \frac{2\mu\epsilon}{\gamma} x \quad (0 < x \leq x_M) \tag{17}$$

To the right of point M, when an insolubles triangle falls onto the SS interface (Fig. 10a), part of the insolubles slip down and is distributed uniformly on the BS

interface (Fig. 10b).

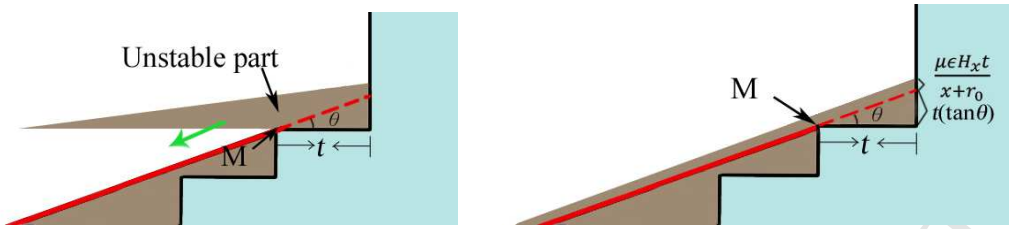

(a) **(b)**

Fig. 10. Increased height of the SS interface to the right of point M in one time step. (a) Before the insolubles slip down. (b) After the insolubles slip down.

The volume of the stable part is $\frac{t^2(\tan\theta)}{2}$, thus the volume of the unstable part is $\mu\epsilon H_x t - \frac{t^2(\tan\theta)}{2}$. Therefore, the increased height of the SS interface in one unit time step can be written as

$$y_{SS}{}^{*} = t(\tan\theta) + \frac{\mu\epsilon H_x t - \frac{t^2(\tan\theta)}{2}}{x+r_0} \tag{18}$$

where $y_{SS}{}^{*}$ is the increased height of the SS interface in one unit time step; r_0 is the distance between the coordinate origin and the symmetry axis of the cavern.

$\frac{t^2(\tan\theta)}{2}$ is a minimum value, which can be eliminated from Eq. (18)

$$y_{SS}{}^{*} = t\left(\tan\theta + \frac{\mu\epsilon H_x}{x+r_0}\right) \tag{19}$$

Therefore, the equation of the SS interface can be expressed as

$$y_{SS}(x) = \begin{cases} \frac{2\mu\epsilon}{\gamma}x & (0 < x \le x_M) \\ y_{SS}(x-t) + t\left(\tan\theta + \frac{\mu\epsilon H_x}{x+r_0}\right) & (x > x_M) \end{cases} \tag{20}$$

where $x_M = \frac{\gamma^2(H_M+H_0)}{8\mu\epsilon\cot\theta - 4\gamma}$.

The slope of the BS interface remains $\tan\theta$, and BS interface intersects SS interface on wall-N, thus the equation of the BS interface is

$$y_{BS} = \tan\theta(x - x_N) + y_N \tag{21}$$

where x_N is the x-coordinate of wall-N; y_N is the y-coordinate of the SS interface on

wall-N.

The roof of the salt cavity will be dissolved as the blanket is raised in the later leaching stages. The insoluble substances contained in the cavern roof will fall down to the BS interface formed in the previous stages. Therefore, the equations of the insolubles accumulation shape should be modified when the dissolution of the cavern roof is considered. In this process, the SS interface has covered by the insoluble sediments, thus the equation of the SS interface will not be influenced. The equation of the BS interface can be calculated by adding the additional part of insoluble substances from the top of the cavern, which is expressed as

$$y_{BS} = \tan\theta(x - x_N) + y_N + \mu\epsilon\Delta H_x \tag{22}$$

where ΔH_x is a variable which represents the height of the additional part of the dissolved cavern roof at x.

The dissolved cavern roof is an inverted funnel shape in most cases, which is higher in the middle. More rock salt is dissolved in the center parts of the cavern roof, and more insoluble particles fall onto the central part of the SS Interface. Therefore the slope of the BS interface will decrease, and the insoluble sediments will not slip down. Eqs. (20) and (22) are the equations of the SS interface and BS interface.

3.3. Numerical solution

In Section 3.2, Eqs. (20) and (22) provide the theoretical formulas of the shape of the SS interface and BS interface of the insoluble sediments. Eq. (20) is a recursion formula, which can be conveniently solved by a computer program. We develop a program by using C++ computer language to obtain the numerical solution of the

equations as shown in Fig. 11. The basic input parameters are θ, t, γ, r_0, x_N, μ, and ϵ. The values of H_x and ΔH_x in each time step can be calculated from the results of the previous step, which are used as input for the next step. Starting from the origin, the equation of the SS interface can be calculated step by step, using Eq. (20). Since y_N can be calculated from the equation of the SS interface, the equation of the BS interface can be calculated by substituting y_N into Eq. (22).

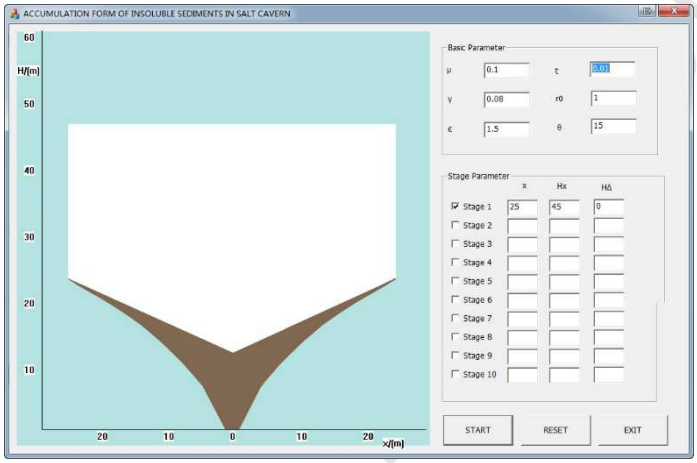

Fig. 11. Window of the program developed by C++ computer language.

Fig. 12 shows the shape of the two interfaces with undissolved (Fig. 12a) and dissolved (Fig. 12b) cavern top, simulation results of the software. When the cavern top is undissolved (Fig. 12a), to the left of point M, the slope of the SS interface is $\frac{2\mu\epsilon}{\gamma}$ (Eq. (20)). To the right of point M, when x increases, the height of the insoluble sediments increases and the height of the cavern side-wall H_x decreases, thus the value of $\frac{\mu\epsilon H_x}{x}$ will decrease. Therefore, the slope of the SS interface will decrease and gradually approach to $\tan\theta$ (Eq. (20)). The BS interface has a constant slope and it shows an inverted cone, which matches the cavern floor shape in most sonar detection observations. When the cavern top is dissolved, the shape of the BS interface is as shown in Fig. 12b. The insoluble sediments in a salt cavern are shaped like the letter

"Y", which explains why the insolubles could be nearly half as high as the whole cavern when its volume is less than 20 percent of the cavern.

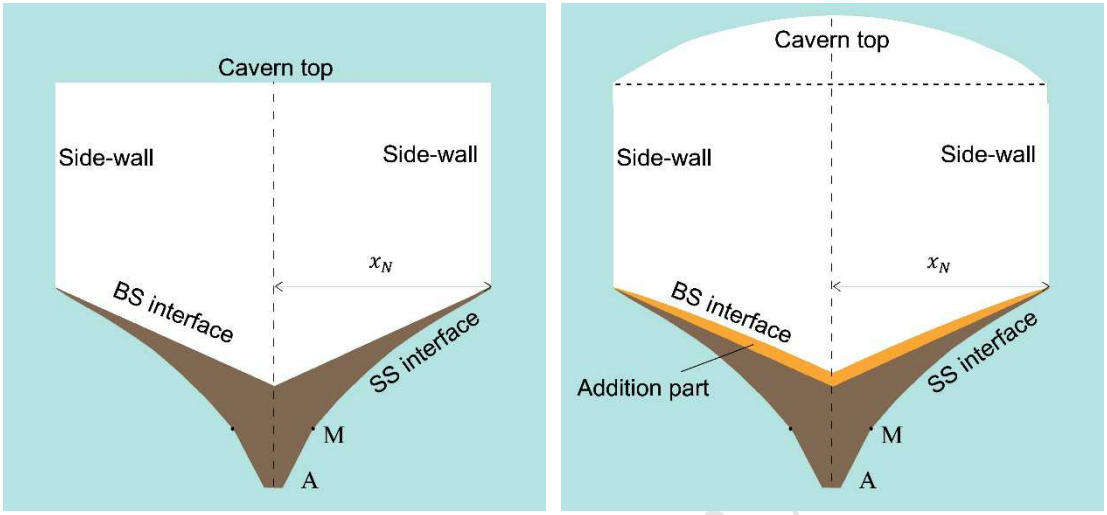

(a) **(b)**

Fig. 12. Shape of the BS interface and the SS interface. (a) Cavern with un-dissolved top. (b) Cavern with dissolved cavern top.

4 Verification and application

To verify the accuracy of the proposed mathematical model, cavern JT-52 of Jintan salt mine is simulated as an example. Cavern JT-52 was created in Jintan salt mine. The cavern shape is roughly axisymmetric, the cavern wall is vertical in the whole leaching process, and there are few large insoluble interlayers over the height range of the cavern, which conform very well with the assumptions of the model. In this section, the actual sonar detection observation of cavern JT-52 will be compared to the simulation results of the C++ program.

Six real sonar detection observations of cavern JT-52 are drawn in Fig. 13a. The BS interface is the actual cavern floor. Connecting the bottom corner of these cavern shapes and the borehole bottom, the SS interface is obtained as well.

Based on the actual geological parameters of cavern JT-52, θ is about 35 degrees, μ is 0.1624, ϵ is 1.5, and r_0 is 0.2. Based on the experiments in Section 2.1, γ is 0.08. In addition, we take t as 0.01 m, input x_N, H_x and ΔH_x in each stage, then six different insolubles accumulation shapes are calculated. The results are drawn on the original sonar image (Fig. 13b).

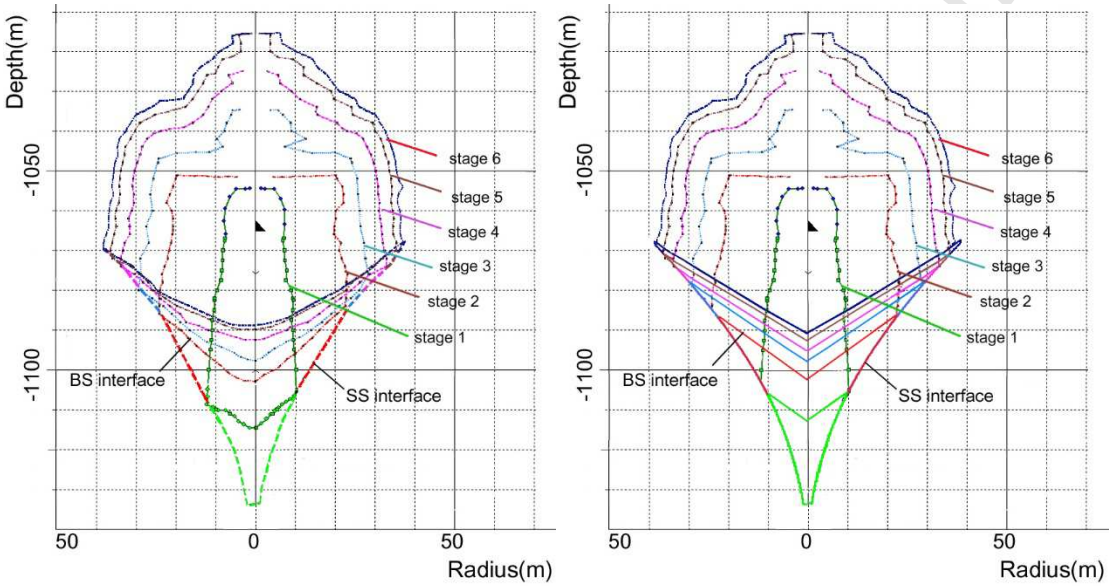

Fig. 13. Comparison between the model simulation and the sonar image of cavern JT-52. (a)Sonar detector observation. (b) Model simulation of insolubles accumulation.

The average errors of the height of the BS interface and SS interface between the measured data and the prediction data are 1.37 m and 0.63 m respectively, which account for about 2.23% and 1.05% of the maximum height of the insoluble sediments in this cavern. It indicates the proposed mathematical model can satisfy the actual engineering requirement. In the initial leaching stage(viz., the depth between -1130 m and -1110 m), the slope of the SS interface is very steep, and the cavern bottom rises up very fast. The reason is that the cavern base area is very small in the initial leaching stage, and the height of the insoluble sediments increases fast. As the

cavern grows and the cavern radius increases, the slope of the SS interface decreases. At depth -1070 m, the slope of the SS interface is 0.65, which is close to the tangent value of the angle of repose of the insoluble sediments (35 degrees). In the center of the cavern, the BS interfaces in the sonar image is smoother than that obtained by the simulations. This results from the fact that the angle of repose of the insoluble sediments is smaller under the effect of brine flow around the leaching tubing.

As shown in Fig. 13, the SS interface rises up fast and there are plenty of rock salt wastes around the SS interface. To improve the utilization rate of rock salt and increase the cavern volume, the leaching parameters are optimized by using the proposed mathematical model. Based on Eq. (20), the slope of the SS interface will decrease faster and there would be more salt being dissolved when the parameters (H_x, μ, and ϵ) have smaller values. However, μ and ϵ are constant and can be ignored in a certain salt bed, which makes H_x a key factor affecting the cavern bottom shape. When we halve the input H_x in the early leaching stages and run the simulation again, the shapes of the new BS interface and SS interface are as shown in Fig. 14. Salt between the old SS interface and the new SS interface can be used effectively due to the decrease of H_x. The capacity of the cavern increases from 187,119 m^3 to about 232,600 m^3 with an increase of 23.77%. To increase the utilization rate of salt beds and the volume of the cavern, a lower distance between the inner leaching tubing and the blanket is suggested in the early leaching stages.

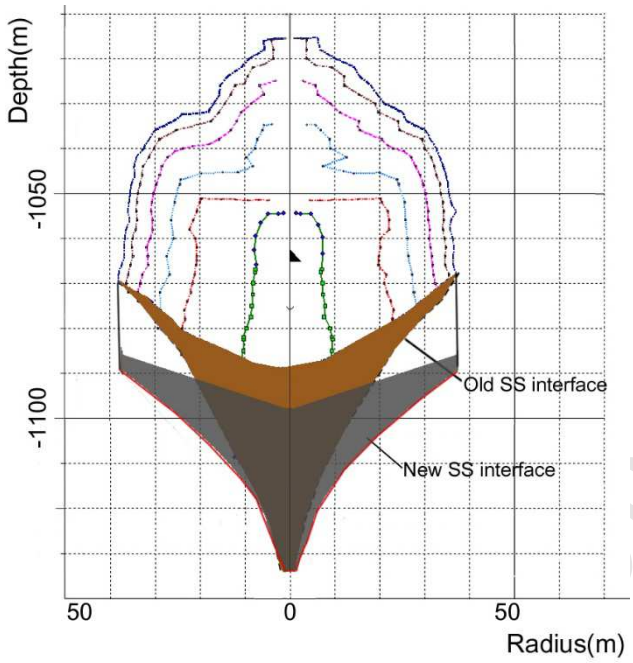

Fig. 14. The accumulation of the insolubles with lower H_x.

5 Conclusions

(i) Insoluble particles falling experiments and rock salt dissolution experiments have been carried out to obtain the properties of the fallen insoluble particles distribution and the influence of the insolubles on the dissolution of the cavern side-wall. Experimental results show that the accumulation shape of the insoluble particles in one time step is approximately a triangle, whose base length is proportional to the height of the cavern wall. Once the rock salt is covered by the insolubles, its dissolution stops.

(ii) The cutoff value of insoluble substances content in rock salt is introduced to build a mathematical model to predict the accumulation shape of the insoluble sediments. The equations of the SS interface and BS interface of the insolubles accumulation shape are derived. The accumulation shape of the insoluble sediments in the salt cavern is mainly affected by the content of the insolubles in rock salt, the

expansion coefficient of the insolubles in brine, and the height of the cavern wall.

(iii) Software is developed based on the theoretical formulas by using C++ computer language. JT-52 cavern of Jintan salt mine is simulated by the program as an example, and the calculated results are compared with the actual sonar survey data. The results show that the mathematical model can satisfy the accuracy requirement of the practical engineering.

(iv) A smaller distance between the inner leaching tubing and the blanket is proposed in the early leaching stages to increase the use efficiency of the salt beds and the cavern capacity.

Acknowledgements

This work is sponsored by the National Natural Science Foundation of China (No. 41472285, No. 51404241, No. 51304187, No. 41272391, No. 41502296) and Youth Innovation Promotion Association CAS (No. 2016296). The authors are sincerely grateful to Jaak J Daemen for his thoughtful review of this paper.

References

Arfaee, M.I.R., Sola, B.S., 2014. Investigating the effect of fracture–matrix interaction in underground gas storage process at condensate naturally fractured reservoirs. Journal of Natural Gas Science and Engineering 19(19), 161-174. DOI: 10.1016/j.jngse.2014.05.007

Charnavel, Y., Lubin, N., 2002. Insoluble deposit in salt cavern - test case. In: Proc of SMRI fall meeting, Bad Ischl, Austria.

Chen, J., Ren, S., Yang, C.H., Jiang, D.Y., Li, L., 2013. Self-healing characteristics of damaged rock salt under different healing conditions. Materials 6, 3438-3450. DOI: 10.3390/ma6083438

Chen, X.Y., Zhang, L., Li, Y.F., Ma, H.L., Ji, G.D., 2013. Experimental investigation on bulking-expansion coefficient of sediment of storage in bedded salt. Mining R&D 33(2), 34-42. (in Chinese).

Durie, R.W., Jessen, F.W., 1964. Mechanism of the dissolution of salt in the formation of underground salt cavities. SPE Journal 4(2), 183-190. DOI: 10.2118/678-PA

Feng, J., Hu, H.H., Joseph, D.D., 1994. Direct simulation of initial value problems for the motion of solid bodies in a Newtonian fluid Part 1. Sedimentation. Journal of Fluid Mechanics. 261. 95-134. DOI: 10.1017/S0022112094002764

Hu, H.H. , Joseph, D.D., Crochet, M.J., 1992. Direct simulation of fluid particle motion. Theoretical and Computational Fluid Dynamics. 3(5), 285-306. DOI: 10.1007/BF00717645

Li, Y.P., Liu, W., Yang, C.H., Daemen, J.J.K., 2014. Experimental investigation of mechanical behavior of bedded rock salt containing inclined interlayer. International Journal of Rock Mechanics and Mining Sciences 69, 39-49. DOI: 10.1016/j.ijrmms.2014.03.006

Liu, W., Li, Y.P., Yang, C.H., Daemen, J.J.K., Yang, Y., Zhang, G.M., 2015. Permeability characteristics of mudstone cap rock and interlayers in bedded salt formations and tightness assessment for underground gas storage caverns. Engineering

Geology 193, 212–223. DOI: 10.1016/j.enggeo.2015.04.010

Ma, H.L., Yang, C.H., Li, Y.P., Shi, X.L., Liu, J.F., Wang, T.T., 2015. Stability evaluation of the underground gas storage in rock salts based on new partitions of the surrounding rock. Environ Earth Sciences 73, 6911–6925. DOI: 10.1007/s12665-015-4019-1

Nolen, J.S., von Hantlemann, O., Meister, S., Kleinitz, W., Heiblinger, J., 1974. Numerical Simulation of the Solution Mining Process. In: SPE European Spring Meeting, Amsterdam, Netherlands. DOI: 10.2118/4850-MS

Quintanilha, J.E., Nguyen-Minh, D., 1994. An approach for optimising an underground hydrocarbon storage field in bedded salt rock formations. Rock Mechanics in Petroleum Engineering. Delft, Netherlands.

Reda, D.C., Russo, A.J., 1986. Experimental Studies of salt-cavity leaching by freshwater injection. SPE Production Engineering 1(1), 82-86. DOI: 10.2118/13308-PA

Shi, X.L., Li, Y.P., Yang, C.H., Xu, Y.L., Ma, H.L., Liu, W., Ji, G.D., 2015. Influences of filling abandoned salt caverns with alkali wastes on surface subsidence. Environmental Earth Sciences 73, 6939-6950. DOI: 10.1007/s12665-015-4135-y

Sobolik, S.R., Ehgartner, B.L., 2006. Analysis of cavern shapes for the strategic petroleum reserve. Albuquerque, USA: Sandia National Laboratories. DOI: 10.2172/888563

Staudtmeister, K., Rokahr, R.B., 1997. Rock mechanical design of storage caverns for natural gas in rock salt mass. Int. J. Mech. Min. Sci. 34, 300. DOI:

10.1016/S1365-1609(97)00199-8

von Tryller, H., Musso, L., 2006. Controlled cavern leaching in bedded salt without blanket in Timpa Del Salto. In: Proc of SMRI spring meeting, Brussels, Belgium.

Wang, T.T., Yan, X.Z., Yang, H.L., Yang, X.J., Jiang, T.T., Zhao, S., 2013. A new shape design method of salt cavern used as underground gas storage. Applied Energy 104, 50-61. DOI: 10.1016/j.apenergy.2012.11.037

Wang, T.T., Yang, C.H., Ma, H.L., Daemen, J.J.K., Wu H.Y., 2015a. Safety evaluation of gas storage caverns located close to a tectonic fault. Journal of Natural Gas Science and Engineering 23, 281-293. DOI: 10.1016/j.jngse.2015.02.005

Wang, T.T., Ma, H.L., Yang, C.H., Shi, X.L., Daemen, J.J.K., 2015b. Gas seepage around bedded salt cavern gas storage. Journal of Natural Gas Science and Engineering 26, 61-71. DOI: 10.1016/j.jngse.2015.05.031

Warren, J.K., 2006. Solution mining and cavern use, in: Evaporites: Sediments, Resources and Hydrocarbons. Springer Berlin Heidelberg, pp. 893-943. DOI: 10.1007/3-540-32344-9_12

Willson, S.M., Driscoll, P.M., Judzis, A., Black, A.D., Martin, J.W., Ehgartner, B.L., 2004. Drilling salt formations offshore with seawater can significantly reduce well costs. SPE Drilling & Completion 19(3), 147-155. DOI: 10.2118/87216-PA

Yang, C.H., Wang, T.T., Li, Y.P., Yang, H.J., Li, J.J., Qu, D.A., 2015. Feasibility analysis of using abandoned salt caverns for large-scale underground energy storage in China. Applied Energy 137, 467-481. DOI: 10.1016/j.apenergy.2014.07.048

Zhang, G.M., Li, Y.P., Yang, C.H., Daemen, J.J.K., 2014. Stability and tightness

evaluation of bedded rock salt formations for underground gas/oil storage. Acta Geotechnica 9(1), 161-179. DOI: 10.1007/s11440-013-0227-6

We propose a prediction model of the insolubles accumulation shape in salt cavern UGS.

Experiments have been carried out to determine the properties of the insolubles.

The equations of the two interfaces of the insolubles accumulation are dirived.

A software has been developed to simulate the insolubles accumulation shape.

Lower the cavern height in early leaching stages will increase the cavern capacity.